Journal of Catalysis **195,** 46–50 (2000)
doi:10.1006/jcat.2000.2959, available online at http://www.idealibrary.com on IDEAL®

Simulation of the Kinetics of Oxidation of Saturated Hydrocarbons on Pt

V. P. Zhdanov*,† and B. Kasemo*

*Department of Applied Physics, Chalmers University of Technology, S-412 96 Göteborg, Sweden; and †Boreskov Institute of Catalysis, Russian Academy of Sciences, Novosibirsk 630090, Russia

Received February 28, 2000; revised May 29, 2000; accepted June 1, 2000

The steady-state kinetics of C_3H_8 oxidation on Pt are calculated assuming the process to be limited by concerted dissociative adsorption of C_3H_8 on vacant sites near adsorbed oxygen atoms (with breaking of a C–H bond and formation of OH). The results, obtained by using (1) the ideal model implying Langmuir adsorption, (2) a model based on the assumption that the saturation oxygen coverage is lower than one monolayer, and (3) a model taking into account adsorbate–adsorbate lateral interactions, indicate that the latter two models can reproduce the apparent reaction orders with respect to C_3H_8 and O_2, observed experimentally under the lean-burn conditions. Model 3 is preferable because its basis is physically more sound.

Key Words: **Langmuir overlayer; nonideal models; adsorbate–adsorbate lateral interactions; reaction orders; lean-burn conditions.**

1. INTRODUCTION

Steady-state kinetics of practically important catalytic reactions are customarily described by using the conventional Hougen–Watson-type equations implying that the entire reaction occurs in the ideal adsorbed overlayer (Langmuir overlayer) via the Langmuir–Hinshelwood or Eley–Rideal mechanism (1). In contrast, the knowledge accumulated in the field of surface science during the past three decades indicates that the kinetics of elementary reaction steps are usually far from ideal due to adsorbate–adsorbate lateral interactions, surface heterogeneity, and/or spontaneous and adsorbate-induced surface restructuring. Incorporation of the latter type of features into the reaction kinetics models is still a challenging problem. Its complexity, reflected in such widely employed terms as *pressure-* and *structure-gap problems*, often derives from the fact that the adsorbate coverages corresponding to practical pressures are much higher than those typical for ultrahigh-vacuum (UHV) conditions, inherent to surface science. Our experience based on simulations of the kinetics of such reactions as hydrogen and CO oxidation on Pt (2, 3) and NO reduction on Rh (4) shows that extrapolation of the reaction kinetics from UHV to atmospheric conditions is hardly possible if one ignores the nonideality of the adsorbed overlayer. In the present paper, we discuss the nonideality of the kinetics of hydrocarbon oxidation on Pt. The understanding of the kinetics of this reaction is of high current interest because hydrocarbons are one of the constituents of exhaust gases. Of special interest is the reaction kinetics during oxygen excess, in view of the legislation-driven trend toward lean combustion.

2. REACTION MECHANISM

As an example, we treat C_3H_8 oxidation,

$$C_3H_8 + 5O_2 \rightarrow 3CO_2 + 4H_2O. \qquad [1]$$

The kinetics of this reaction was recently studied in detail by Burch and Watling (BW) (5) in the case when it occurs in parallel with NO reduction on Pt/Al_2O_3 under lean-burn conditions in a flow reactor. Typical C_3H_8, NO, and O_2 concentrations in He were 200–3000 ppm, 200–2000 ppm, and 1–10%, respectively. Significant C_3H_8 conversion was found at temperatures above 500 K. Analyzing their experimental data, BW conclude that C_3H_8 oxidation is limited by C_3H_8 chemisorption accompanied by breaking of one of the C–H bonds formed by the central carbon atom. This process is assumed to occur in a concerted way on a vacant site near an adsorbed oxygen atom and to result in the formation of OH,

$$(CH_3–CH_2–CH_3)_{gas} + O_{ad} \rightarrow (CH_3–CH–CH_3)_{ads} + (OH)_{ad}.$$

Subsequent reaction steps (after breaking the first C–H bond) are believed to be rapid. Thus, adsorbed atomic oxygen is considered to be the dominant species under the reaction conditions.

Concerted $CH_3–CH_2–CH_3$ chemisorption with the formation of $(OH)_{ad}$ seems to be more plausible compared to chemisorption resulting in the formation of H_{ad}, because the O–H bond is probably much stronger than the H–Pt bond. Actually, a $CH_3–CH_2–CH_3$ molecule may first be trapped into a physisorbed state and then dissociate. From

0021-9517/00 $35.00

the point of view of the formal kinetics, the latter detail does not, however, matter.

We focus our attention on the situation when process [1] is not complicated by other reactions. Treating this case, we accept the reaction mechanism proposed by BW (5). Our goal is to scrutinize and compare the steady-state reaction kinetics predicted for this mechanism, respectively, by the Langmuir and BW models and by our model which takes into account adsorbate–adsorbate interactions.

3. GENERAL BALANCE EQUATION

If C_3H_8 oxidation is complete and oxygen desorption is negligible (the latter is the case if the temperature is not too high, i.e., ≤700–800 K), the steady-state balance of adsorbed species is described as

$$W^{\mathrm{ad}}_{\mathrm{O}_2} = 5W^{\mathrm{ad}}_{\mathrm{C_3H_8}}, \qquad [2]$$

where $W^{\mathrm{ad}}_{\mathrm{O}_2}$ and $W^{\mathrm{ad}}_{\mathrm{C_3H_8}}$ are the adsorption rates of O_2 and C_3H_8, respectively. The factor 5 in the right-hand part of this equation takes into account that one needs five O_2 molecules in order to convert one C_3H_8 molecule to CO_2 and H_2O.

Following BW (5), we assume that the surface is covered primarily by atomic oxygen. The coverages of other species (including the coverage of the propyl fragment) are considered to be negligibly low.

Solving Eq. [2] with explicit expressions for the O_2 and C_3H_8 adsorption rates, we can calculate the reaction rate, which is identified below with the rate of oxygen adsorption, i.e., $W_{\mathrm{r}} \equiv W^{\mathrm{ad}}_{\mathrm{O}_2}$.

4. MODEL 1 (LANGMUIR OVERLAYER)

If adsorbed oxygen atoms are treated as Langmuir particles (i.e., as the lattice gas with no lateral interactions), Eq. [2] is represented as

$$k^{\mathrm{ad}}_{\mathrm{O}_2} P_{\mathrm{O}_2}(1-\theta)^2 = 5k^{\mathrm{ad}}_{\mathrm{C_3H_8}} P_{\mathrm{C_3H_8}}\theta(1-\theta), \qquad [3]$$

where θ is the oxygen coverage (the coverages of other species are neglected), $k^{\mathrm{ad}}_{\mathrm{O}_2}$ and $k^{\mathrm{ad}}_{\mathrm{C_3H_8}}$ are the coverage-independent adsorption rate constants, and P_{O_2} and $P_{\mathrm{C_3H_8}}$ are the reactant pressures.

From Eq. [3], one can easily obtain that the oxygen coverage is given by

$$\theta = 1 - p, \qquad [4]$$

where

$$p = \frac{5k^{\mathrm{ad}}_{\mathrm{C_3H_8}} P_{\mathrm{C_3H_8}}}{k^{\mathrm{ad}}_{\mathrm{O}_2} P_{\mathrm{O}_2} + 5k^{\mathrm{ad}}_{\mathrm{C_3H_8}} P_{\mathrm{C_3H_8}}} \qquad [5]$$

is the relative C_3H_8 impingement rate used hereafter as a governing parameter. For the reaction rate, normalized here and below to $k^{\mathrm{ad}}_{\mathrm{O}_2} P_{\mathrm{O}_2} + 5k^{\mathrm{ad}}_{\mathrm{C_3H_8}} P_{\mathrm{C_3H_8}}$, one accordingly has

$$W_{\mathrm{r}} = (1-p)p^2. \qquad [6]$$

5. MODEL 2 (MODIFIED LANGMUIR OVERLAYER)

Under the lean-burn conditions, $p \ll 0.1$, the model implying Langmuir adsorption (Eqs. [4]–[6]) predicts that the reaction orders with respect to C_3H_8 and O_2 are $+2$ and -1, respectively. In contrast, the experiment (5) indicates that the reaction orders are about $+1$ and 0. To accommodate this disagreement, BW (5) slightly modified the ideal model. In particular, assuming the saturation oxygen coverage, $\theta_{\max}$, to be a little lower than unity, they have postulated that the rate of oxygen adsorption is proportional to $(1-\theta)(\theta_{\max}-\theta)$ (the C_3H_8 adsorption was considered to be described as in the Langmuir model). With this modification, Eqs. [3], [4], and [6] are replaced by

$$k^{\mathrm{ad}}_{\mathrm{O}_2} P_{\mathrm{O}_2}(1-\theta)(\theta_{\max}-\theta) = 5k^{\mathrm{ad}}_{\mathrm{C_3H_8}} P_{\mathrm{C_3H_8}}\theta(1-\theta), \qquad [7]$$

$$\theta = (1-p)\theta_{\max}, \qquad [8]$$

$$W_{\mathrm{r}} = p(1-p)[(1-p)(1-\theta_{\max}) + p]\theta_{\max}. \qquad [9]$$

Under the lean-burn conditions, one has $W_{\mathrm{r}} \approx p(1-\theta_{\max})\theta_{\max}$. The C_3H_8 and O_2 reaction orders, $+1$ and 0, predicted by the latter expression are in agreement with the experiment. To fit the experimental data, BW employed $\theta_{\max} = 0.994$.

6. MODEL 3 (WITH LATERAL INTERACTIONS)

Despite the apparent agreement with experiment, there is no guarantee that the coverage dependences of the O_2 and C_3H_8 adsorption rates, used by BW, correspond to reality. For example, the physical meaning of the obtained value of the saturation oxygen coverage is not clear. Concerning this point, it is appropriate to note that under UHV conditions the saturation coverages for oxygen adsorption are usually related to the formation of ordered structures in the adsorbed overlayer. On Pt(111), for example, oxygen forms a $p(2\times 2)$ structure at $\theta = 0.25$ ML with adsorption on fcc-hollow sites (6). The saturation oxygen coverage observed in conventional UHV measurements is accordingly 0.25 ML. Practically, this means that at $\theta > 0.25$ the O_2 sticking coefficient decreases with increasing oxygen coverage so rapidly that the rate of oxygen adsorption becomes negligibly low under UHV conditions. This does not mean that adsorption at $\theta > 0.25$ is impossible. Higher coverages can be reached at high pressures or using special methods (7). On the (1×1) Pt(100) surface, the saturation oxygen coverage is about 0.6 (8). Thus, the surface science studies clearly indicate that the coverage dependence of the sticking coefficient for O_2 adsorption on the (111) and (100) faces of Pt is far from Langmuirian at $\theta > 0.25$ and 0.6 ML, respectively. In contrast, the BW model predicts (see Fig. 2 below) that

the O_2 sticking coefficient is nearly Langmuirian almost up to $\theta = 1$.

Although the above information provided by surface science studies is not sufficient to simulate the kinetics of C_3H_8 oxidation with no fitting parameters, it at least allows an estimate of the magnitude of the effects modifying the Langmuir kinetics of O_2 and C_3H_8 adsorption at relatively high coverages.

Physically, the rapid decrease of the O_2 sticking coefficient observed on Pt(111) or (100) at $\theta > 0.25$ and 0.6 ML is connected with adsorbate–adsorbate lateral interactions. In general, one should distinguish between lateral interactions in the ground and activated states (9) (the terms "ground" and "activated" correspond here to the transition state theory). The former interactions, affecting the energy level of the bottom of the adsorption potential well, result in ordering of adsorbed oxygen atoms. The latter ones, shifting the energy of the saddle point, are manifested only in the kinetics of O_2 adsorption. To illustrate the effect of these interactions, we assume for simplicity that adsorption occurs on a square lattice (Fig. 1), take into account only interactions between nearest-neighbor (nn) particles, and use the quasi-chemical (QC) approximation in order to describe the oxygen ordering.

Considering that O_2 molecules adsorb dissociatively on pairs of vacant nn sites, we have the following general expression for the rate of oxygen adsorption (9),

$$W_{O_2}^{ad} = k_{O_2}^{ad} P_{O_2} \sum_i \mathcal{P}_{00,i} \exp(-\epsilon_i^*/k_B T), \qquad [10]$$

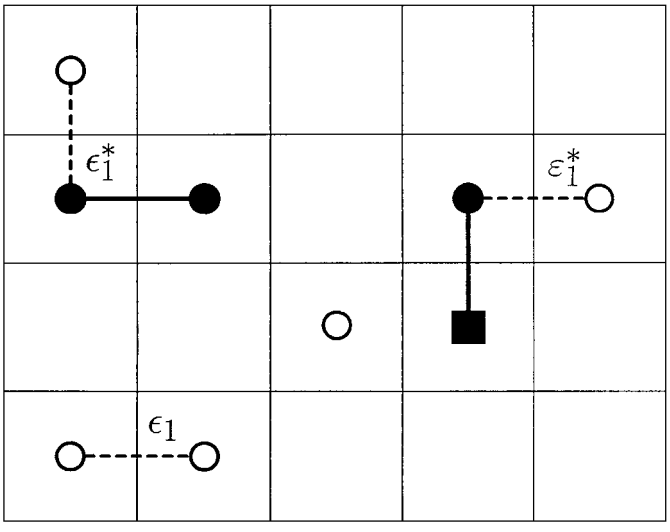

FIG. 1. Schematic arrangement of adsorbed particles on the lattice. Open circles show oxygen atoms. The dimer composed of filled circles represents the activated complex for O_2 adsorption. The dimer consisting of a filled square and a filled circle represents the activated complex $[O–(C_3H_8)]^*$ for C_3H_8 adsorption [the circle and square represent O^* and $(C_3H_8)^*$, respectively]. The dashed lines indicate lateral adsorbate–adsorbate interactions.

where $k_{O_2}^{ad}$ is the adsorption rate constant at low coverages, $\mathcal{P}_{00,i}$ the probability that two nn sites are vacant and that the arrangement of oxygen atoms around this pair of sites is i (i is the index marking the arrangements), and ϵ_i^* the lateral interactions of the activated complex, $(O_2)^*$, with adjacent oxygen atoms.

In our model, the activated complex for O_2 adsorption has six nn sites (Fig. 1). Taking into account lateral interaction of the activated complex with oxygen atoms located in these sites, we have $\epsilon_1^* = n\epsilon_1^*$, where ϵ_1^* is the nn interaction in the activated state, and $n \leq 6$ is the number of nn oxygen atoms. Substituting this expression into Eq. [10] and employing the QC approximation in order to calculate the probabilities of different arrangements of oxygen atoms, we obtain (9)

$$W_{O_2}^{ad} = k_{O_2}^{ad} P_{O_2} \mathcal{P}_{00} S^6, \qquad [11]$$

where

$$S = \frac{\mathcal{P}_{00} + 0.5\mathcal{P}_{A0} \exp(-\epsilon_1^*/k_B T)}{\mathcal{P}_{00} + 0.5\mathcal{P}_{A0}} \qquad [12]$$

is the factor describing the nonideality of adsorption, and $\mathcal{P}_{00}$ and $\mathcal{P}_{A0}$ are the QC probabilities that a pair of nn sites is, respectively, vacant or occupied by one oxygen atom (these probabilities, defined by Eqs. [3.3.22]–[3.3.24] in Ref. (9), depend on the nn O–O interaction in the ground state, ϵ_1). The power 6 in Eq. [11] is related to the number of sites adjacent to the two sites occupied by the activated complex $(O_2)^*$.

Assuming C_3H_8 adsorption to occur on a vacant site near an adsorbed oxygen atom so that the activated state includes this atom, we have (9) (cf. Eq. [10])

$$W_{C_3H_8}^{ad} = k_{C_3H_8}^{ad} P_{C_3H_8} \sum_i \mathcal{P}_{0A,i} \exp[-(\varepsilon_i^* - \epsilon_i)/k_B T], \qquad [13]$$

where $k_{C_3H_8}^{ad}$ is the coverage-independent rate constant; $\mathcal{P}_{0A,i}$ the probability that a vacant site has an nn site occupied by oxygen and that the arrangement of oxygen atoms around this pair of sites is i; ϵ_i the interaction (before reaction) of the oxygen atom, participating in the reaction, with other oxygen atoms belonging to configuration i; and ε_i^* the lateral interactions of the activated complex $[O–(C_3H_8)]^*$ with adjacent oxygen atoms.

For C_3H_8 adsorption, the activated complex, $[O–(C_3H_8)]^*$, is not symmetric (Fig. 1), and accordingly we need in general to introduce two lateral nn interactions in the activated state, corresponding respectively to $O–O^*$ and $O–(C_3H_8)^*$ pairs (O is the nonactivated oxygen atom, and O^* and $(C_3H_8)^*$ are the fragments of the activated complex). To reduce the number of model parameters, we take into account only the $O–O^*$ interaction, ε_1^*, as shown in Fig. 1 (note that in general $\varepsilon_1^* \neq \epsilon_1^*$). In this case, the rate of C_3H_8 adsorption calculated in the QC approximation is

represented as (9)

$$W^{ad}_{C_3H_8} = k^{ad}_{C_3H_8} P_{C_3H_8} 0.5 \mathcal{P}_{A0} V^3, \qquad [14]$$

where

$$V = \frac{\mathcal{P}_{AA} \exp[-(\varepsilon_1^* - \epsilon_1)/k_B T] + 0.5\mathcal{P}_{A0}}{\mathcal{P}_{AA} + 0.5\mathcal{P}_{A0}}. \qquad [15]$$

The power 3 in Eq. [14] is related to the number of sites for O adsorption near O* [this number is smaller than 4, because one of the nn sites is occupied by $(C_3H_8)^*$].

7. RESULTS OF CALCULATIONS

Typical values of lateral interactions between nn oxygen atoms on such metals as Pt, Pd, and Rh are 3–4 kcal/mol (4, 9). Lateral interaction in the activated state is usually lower than that in the ground state. In our simulations, we employ $\epsilon_1 = 3$, $\epsilon_1^* = 2$, and $\varepsilon_1^* = 2$ kcal/mol as probable values. Using these interactions, we have calculated the rates

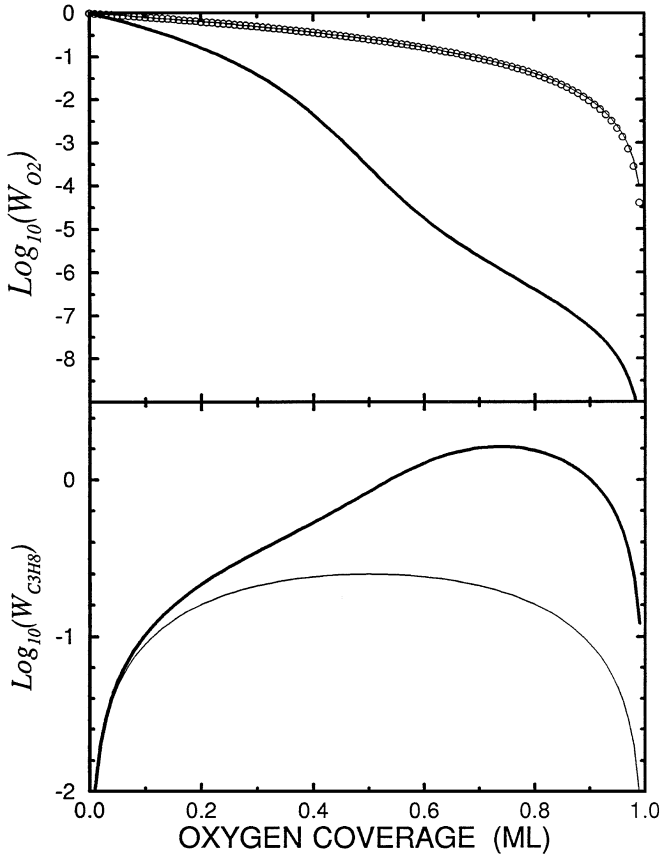

FIG. 2. O_2 and C_3H_8 adsorption rates (normalized to $k^{ad}_{O_2} P_{O_2}$ and $k^{ad}_{C_3H_8} P_{C_3H_8}$, respectively) as a function of oxygen coverage for $\epsilon_1 = 3$, $\epsilon_1^* = 2$, and $\varepsilon_1^* = 2$ kcal/mol at $T = 600$ K. Thin lines are for model 1 implying Langmuir oxygen adsorption. Circles and thick lines correspond, respectively, to model 2 proposed by BW and model 3 taking into account adsorbate–adsorbate lateral interactions.

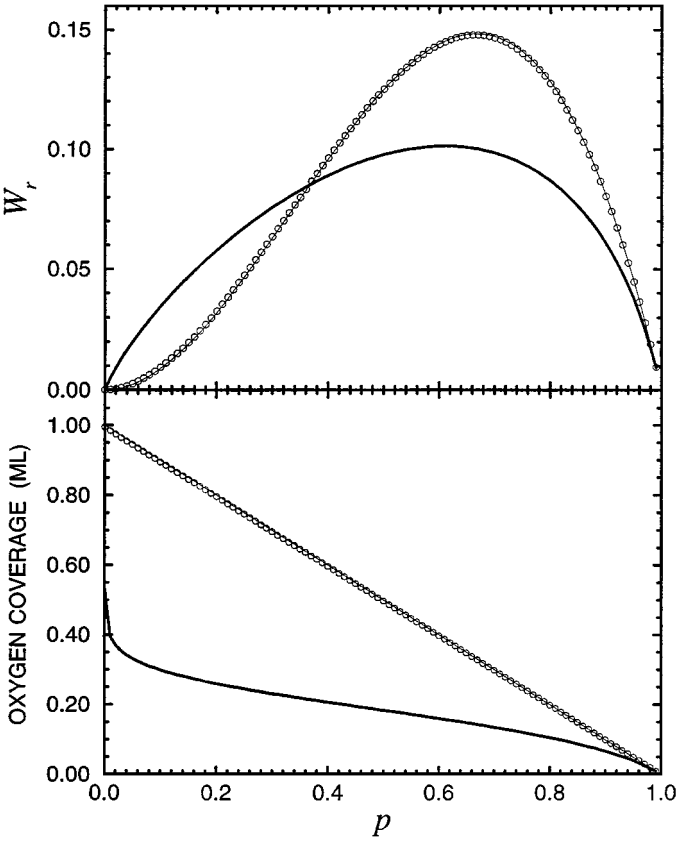

FIG. 3. Reaction rate (normalized to $k^{ad}_{O_2} P_{O_2} + 5k^{ad}_{C_3H_8} P_{C_3H_8}$) and oxygen coverage as a function of p at $T = 600$ K for model 1 implying Langmuir adsorption (thin lines), model 2 proposed by BW (circles), and model 3 taking into account adsorbate–adsorbate lateral interactions (thick lines). The parameters are the same as in Fig. 2.

of O_2 and C_3H_8 adsorption as a function of oxygen coverage and then, employing Eq. [2], the rate of C_3H_8 oxidation as a function of p (the latter rate was normalized to $k^{ad}_{O_2} P_{O_2} + 5k^{ad}_{C_3H_8} P_{C_3H_8}$). The results obtained were compared with those predicted by models 1 and 2 (Sections 4 and 5), ignoring adsorbate–adsorbate lateral interactions.

With increasing oxygen coverage, the rates of O_2 and C_3H_8 adsorption (Fig. 2), calculated with lateral interactions, become respectively much lower and higher than those corresponding to models 1 and 2. A difference between models 1 and 2 is observed (for O_2 adsorption) only at $\theta \to 1$.

The dependences of the steady-state reaction rate and oxygen coverage on p, calculated with lateral interactions at $p \geq 0.01$ (Fig. 3), are quite different compared to those predicted by models 1 and 2 as well. The difference between models 1 and 2 is here negligible.

Under the lean-burn conditions (e.g., $p \leq 10^{-3}$), as already noted, model 1 predicts that the reaction order with respect to C_3H_8 is $+2$ (Fig. 4). Model 2 indicates that the reaction order is $+1$. Model 3 predicts $\simeq +1$ as well. For the reaction order with respect to O_2, the three models yield

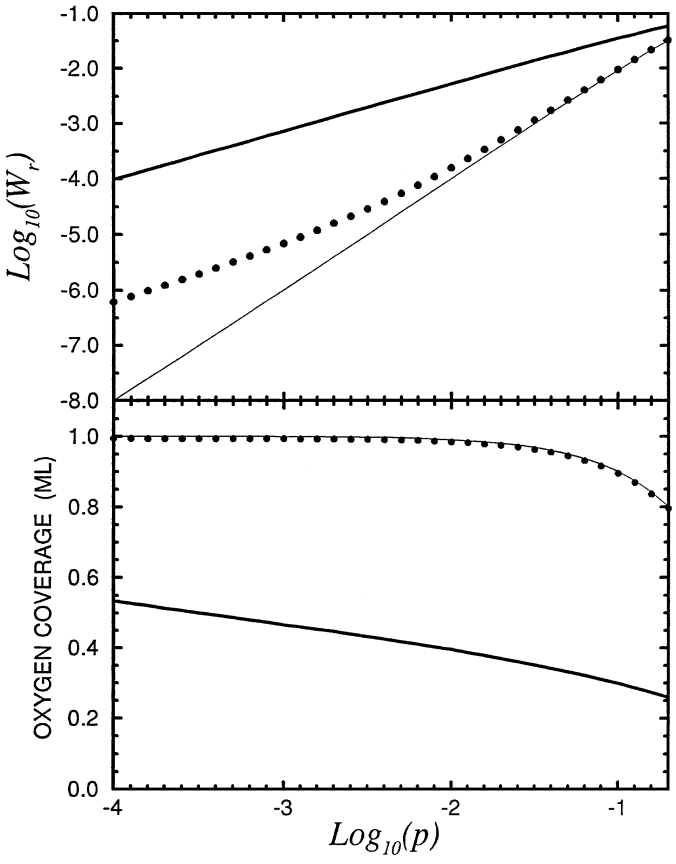

FIG. 4. As Fig. 3 but for the lean-burn conditions.

-1, $\simeq 0$, and $\simeq 0$, respectively. Thus, under the lean-burn conditions, models 2 and 3 result in nearly the same reaction orders. For this reason, model 3 can also be used to describe the experimental data reported in Ref. (5). (The values of the normalized reaction rates corresponding to models 2 and 3 are different at $p \ll 0.1$, but this difference can easily be compensated by choosing appropriate values of the rate constants $k^{\mathrm{ad}}_{\mathrm{O}_2}$ and $k^{\mathrm{ad}}_{\mathrm{C}_3\mathrm{H}_8}$.)

8. CONCLUSION

According to model 2 proposed by BW, the reaction order with respect to C_3H_8 is nearly $+1$ at $p \leq 10^{-3}$ because in this limit the oxygen coverage is close to the saturation coverage which is slightly lower than unity. In contrast, our model (with lateral interactions) predicts (Fig. 3) that the oxygen coverage is far from saturation (at least at $p > 10^{-5}$). The unity reaction order with respect to C_3H_8, observed in our case at $p \leq 10^{-3}$, is connected with the nonideality of the O_2 and C_3H_8 adsorption kinetics due to adsorbate–adsorbate interactions. The latter reason seems physically to be the most likely. Thus, one can expect that our model is applicable over a wider range of reaction conditions. To discriminate experimentally between the two models, one needs to study the C_3H_8 oxidation kinetics over a larger interval of pressures than in Ref. (5) for the situation when the reaction is not complicated by other reactions.

In summary, we have explicitly shown how to incorporate adsorbate–adsorbate lateral interactions into the kinetic models of oxidation of saturated hydrocarbons. The results obtained are expected to be instructive for the understanding and further development of kinetic models of hydrocarbon oxidation, especially in oxygen excess, on such catalytically active metals as Pt, Pd, and Rh. In our treatment, adsorption was assumed to occur on a square lattice and the lateral interactions were considered to be limited by nn pairs. Generalization of our approach on the cases of adsorption on other lattices and/or next-nearest-neighbor (nnn) lateral interactions is straightforward. If for example the nnn interactions are relatively weak, one can combine the QC equations above with the mean-field corrections taking into account the latter interactions, as described in Ref. (10). If the nn and nnn interactions are strong, one should use Monte Carlo simulations in order to calculate the probabilities of arrangement of adsorbed particles.

ACKNOWLEDGMENTS

The authors thank Prof. J. W. Niemantsverdriet for useful comments concerning the presentation of the results. This work is supported by INTAS (Grant No. 97-11720) and the NUTEK Competence Center for Catalysis (Grant No. 4F7-97-10929).

REFERENCES

1. Mezaki, R., and Inoue, H., "Rate Equations of Solid-Catalyzed Reactions." Univ. of Tokyo, Tokyo, 1991.
2. Fassihi, M., Zhdanov, V. P., Rinemo, M., Keck, K.-E., and Kasemo, B., *J. Catal.* **141**, 438 (1993).
3. Zhdanov, V. P., and Kasemo, B., *Appl. Surf. Sci.* **74**, 147 (1994).
4. Zhdanov, V. P., and Kasemo, B., *Surf. Sci. Rep.* **29**, 31 (1997).
5. Burch, R., and Watling, T. C., *J. Catal.* **169**, 45 (1997).
6. Matter, N., Starke, U., Barbieri, A., Döll, R., Heinz, K., Van Hove, M. A., and Somorjai, G. A., *Surf. Sci.* **325**, 207 (1995).
7. Parker, D. H., Bartram, M. E., and Koel, B. E., *Surf. Sci.* **217**, 489 (1989).
8. Griffiths, K., Jackman, T. E., Davies, J. A., and Norton, P. R., *Surf. Sci.* **138**, 113 (1984).
9. Zhdanov, V. P., "Elementary Physicochemical Processes on Solid Surfaces," Chap. 4. Plenum, New York, 1991.
10. Zhdanov, V. P., *Surf. Sci.* **133**, 469 (1983).